Development and Experiment of Electromagnetic Pulse Crimping System for Terminal-Wire of Electric Vehicles

Y. Zhou[1,2*], C. Li[1], T. Shen[1], B. Zhang[1], H. Wu[1], M. Dai[1], X. Wang[1]

[1] State Key Laboratory of Power Transmission Equipment and System Security and New Technology, School of electrical engineering, Chongqing University, Chongqing, 400044 China
[2] Chongqing College of Electronic Engineering, China
*Corresponding author. Email: zhouyan1992@cqu.edu.cn; Tel.: +86 182 905 77146

Abstract

The safety and reliability of the energy transmission system of electric vehicles (EVs) are decided by the connection reliability of the high-voltage (HV) wire harness and terminals. When the terminal and the HV wire harness are connected by the usual mechanical crimping methods such as hydraulic pressure, there are the edges and corners on the terminal, and gaps between the wire harness and terminal, which are prone to fretting corrosion and threaten the power system. In this work, an electromagnetic pulse crimping (EMPC) system has been designed and developed for joining the Cu wire harness and the Cu terminal of the EV. When the discharge voltage is 13 kV, it can deliver the discharge current of 70 kA peak value, causing the joint of the Cu terminal and the Cu HV wire harness. Scanning electron microscope (SEM) and energy dispersive spectrometer (EDS) were used to analyze the microstructure and element distribution of the joint interface. A good and strong metallurgical bond was obtained at the surface of the Cu HV wire harness, the Cu terminal, and each strand of the Cu HV wire harness. There were a flat interface and a wavy interface between the Cu HV wire harness and the Cu terminal because of the gap on the field shaper.

Keywords

HV wire harness, Terminals, Electric vehicles, Electromagnetic pulse crimping

1 Introduction

Electric vehicle (EV) is driven by electric energy without producing carbon dioxide and toxic gases, which could reduce the dependence on fossil energy, so it is one of the main development directions of transportation (Lopes et al. 2011). And the demand for EVs continues to grow (Engr et al. 2020). The high-voltage (HV) wire harness plays an important role because it connects the battery and the power unit of the EVs, which is used to transmit the electric energy of the battery to each subsystem. Therefore, the joint of the HV wire harness and terminal must meet the working conditions of HV and large current transmission.

In the using process of HV terminal-wire joint, the high temperature is created by the high current then the elasticity of the contact is decreased after heating, or an insulating metal oxide film is formed in the contact area of the joint, reducing contact reliability, increasing contact resistance, and further increasing the temperature, which leads to impotent contact and threatens the safety of EVs. Thus, the reliability of the connection between the HV wire harness and the terminal is very important. At present, the main method is mechanical crimping, but when the tool turns loose, the terminal rebounds, causing a gap between the wire harness and the terminal contact interface, which leads to increased resistance and energy loss in the contact area. Moreover, the uneven deformation of the mechanical crimping terminal, the material extrusion at the contact interface between the crimping tool and the terminal, and the gap between the wire strands make it difficult for the joint to meet the connection requirements of the HV wire harness and the terminal (Rajak and Kore, 2018). Therefore, there is an urgent need for a new technology for reliably connecting terminals and HV wire harnesses, which has important practical significance and engineering value.

Electromagnetic pulse forming (EMPF) technology is a kind of pulse power technology in the application of material processing (Psyk et al., 2011). It uses a strong pulse magnetic field to act on a metal workpiece to produce a high-speed and large-scale deformation. This technology has some advantages of a fast forming process and no spring-back. Also, it can increase the forming limit of metal materials, environmental protection, and energy controllable. Moreover, this technology can also be used to weld dissimilar metals, including tube welding and plate welding. The welding process of the copper tubes and steel tubes had been investigated by Shotri et al. (2020). Itoi et al. (2019) welded the 6061 aluminum alloy plate and DP590 steel plate by the EMPF. Zhou et al. (2021) used the EMPF to connect Cu plates and Al plates.

Therefore, this work proposes the use of EMPF technology to crimp the HV wire harness and the terminal for EVs. An electromagnetic pulse crimping (EMPC) system was built for HV wire harnesses based on the structural characteristics of HV wire harnesses and terminals. Crimping experiments of Cu HV wire harnesses and Cu terminals were carried out. Scanning electron microscope (SEM) and energy dispersive spectrometer (EDS) were used to explore the bonding mechanism of the HV wire harness and the terminal.

2 Method and Materials

2.1 EMPC system

An EMPC system consisting of a 140 μF/20 kV/28 kJ capacitor bank was designed and built. The schematic diagram of the EMPC system is shown in Fig. 1. The system consists of a capacitor bank, multi-pole vacuum trigger (MTVS), high-voltage (HV) power supply, trigger source, coil, and field shaper. Transmission copper plates are used to connect the capacitor bank and discharge switch. The MTVS is used as the discharge switch because it can work at the condition of higher voltage and larger current. The MTVS is controlled by the 5 kV/5 μs trigger signal produced by the trigger source (Zhou et al. 2017). Four numbers of coaxial cables are used to connect the MTVS to the coil, which can reduce the stray parameters of the discharge circuit. The capacitor bank is charged through a 20 kV/30 mA HV power supply. The capacitor bank and its power supply are isolated using a vacuum relay (charging switch) after charging it to the rated voltage. A drain circuit is installed on the side of the capacitor bank, including a drain switch and a resistor. After each crimping process, the drain switch is turned on and the residual voltage of the capacitor bank is dropped to zero. The discharge switch, charge switch, and drain switch are controlled by an STM 32.

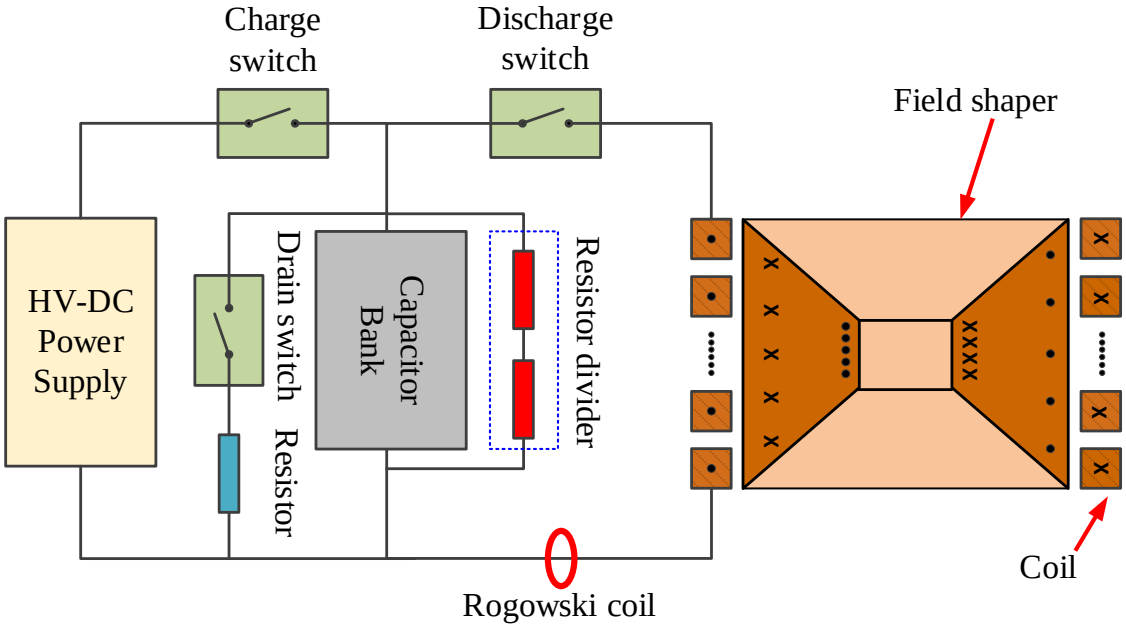

***Figure 1**: The schematic diagram of the EMPC system*

2.2 Measurement method

The discharge voltage (charge voltage) of the capacitor bank is monitored with a resistor divider of 400:1 attenuation, and the discharge current is measured with an integrated

Rogowski coil of 1 V/200 kA sensitivity. The voltage and current signals are collected by the capture card and displayed on the computer screen. After crimping, a scanning electron microscope (SEM) TM4000Plus II is used to perform line scan and surface scan on the bonding interface of the crimped sample. The element distribution is also analyzed by EDS. The surface temperature of the Cu terminal coating is measured by an infrared thermometer.

2.3 Materials

The crimping samples are shown in Fig. 2. Fig. 2(a) is the Cu HV wire harness with a coaxial structure. The transmission layer consists of 12 strands of wire bundles. Each wire bundle contains copper wires with a diameter of 0.46 mm. The radius of the transmission layer is about It is 6.71 mm. Fig. 2(b) is a Cu terminal with an outer diameter of about 19.05 mm and an inner diameter of about 14.03 mm. The contact area of the terminal is about 19.13 mm. From the inside to the outside, there are Sn coating and Ag coating on the surface of the Cu terminal.

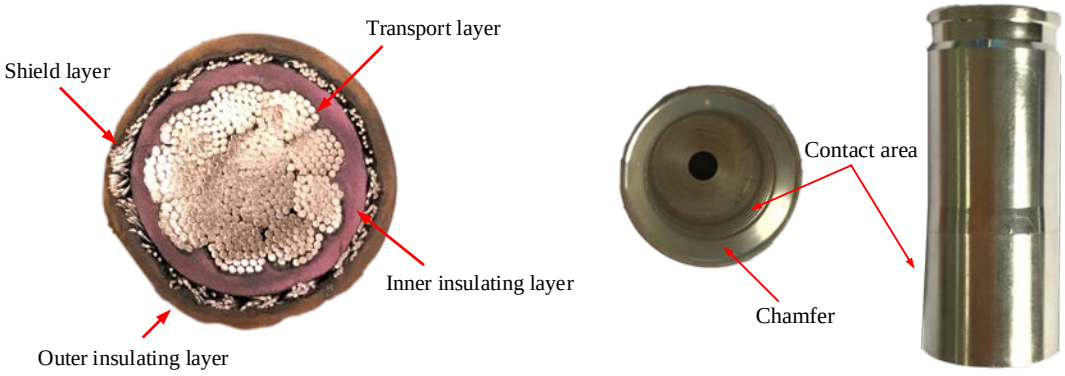

***Figure 2**: (a) Cu HV wire harness, and (b) Cu terminal*

3 Discharge current and temperature

The thickness of the Cu terminal is about 2.5 mm, which requires high energy to deform it. In the experiment, the discharge voltage started from 10 kV and increased in steps of 1 kV. When the discharge voltage is 10 kV, the Cu terminal undergoes plastic deformation with deformation of about 0.72 mm, but it is not tightly combined with the HV wire harness and it is easy to fall off. When the discharge voltage is 13 kV, the Cu terminal and the HV wire harness form a close combination. At this time, the discharge voltage and discharge current are shown in Fig. 3. When the discharge switch is turned on, the voltage of the capacitor bank begins to drop and the discharge current begins to increase. After 45 μs, the discharge current reaches its peak value, which is about 70 kA. The discharge current waveform is not a continuous RLC attenuated oscillation wave, and it is cut off after about two and a

half cycles. The MTVS has cut-off characteristics. When the discharge current change rate is low, the MTVS turns off. The short circuit discharge frequency of the system is about 5.6 kHz.

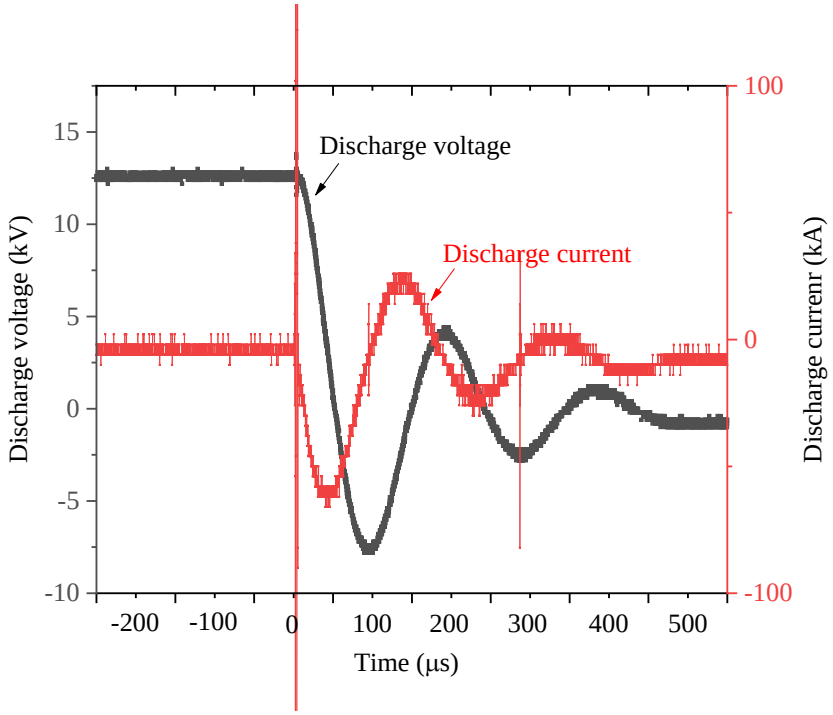

***Figure 3**: Waveforms of discharge voltage and discharge current*

The skin depth of the Cu terminal δ is given as

$$\delta = \frac{1}{\sqrt{\mu \pi f \sigma_e}} \tag{1}$$

where μ is the relative permeability and σ_e is the electrical conductivity. When the discharge frequency is about 5.6 kHz, the skin depth of the discharge current in the Ag coating layer is about 1 μm. Therefore, the discharge current is mainly concentrated on the Ag coating layer.

When the induced eddy current flows through the Cu terminal, the heat source Q caused by the Joule heating can be obtained by Eq. 1 given by Cao et al. (2015).

$$Q = \frac{1}{\sigma_e} \boldsymbol{J} \times \boldsymbol{J} \tag{2}$$

where $\boldsymbol{J}$ is the induced eddy current of the terminal. During the crimping process, the surface temperature of the Cu terminal increases with the increase of the discharge voltage. When the discharge voltage is 13 kV, the surface temperature rise of the Cu terminal is about 35 °C, which is lower than the melting point of Ag (961 °C). Thus, there is no obvious effect on the surface of the coating when the temperature rise of the Cu terminal is caused by crimping.

4 Connection interface and element distribution

4.1 Macromorphology analysis

The crimped joint of the HV wire harness and terminal is shown in Fig. 4(a), and the surface of the joint area is still smooth, without wrinkles, burrs, edges, or corners. The diameter D_1 of the joint changes from 19.05 mm to 17.52 mm, and the compression rate is about 85%. During the crimping process, the outer surface coating layer was not damaged. At the chamfer of the terminal, the terminal completely wraps and covers the wire harness. Wire cutting was used to cut the mark of the sample in Fig. 4(a), and the macroscopic morphology of the crimping cross-section is shown in Fig. 4(b). In most areas of the cross-section, there is no obvious boundary between the HV wire harness and the Cu terminal, which shows a metallurgical bond has been formed. And there is also no obvious boundary between the Cu wire harness and the Cu wire harness, forming a whole.

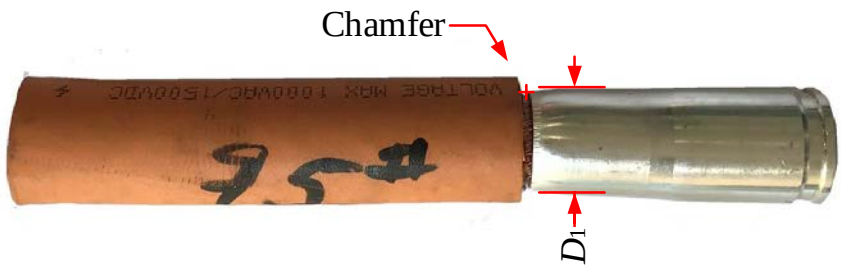

(a)

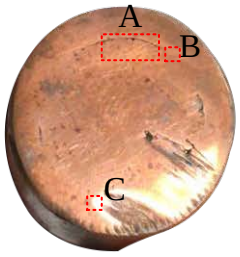

(b)

Figure 4*: (a) Crimped sample of Cu HV wire harness and Cu terminal, and (b) Cross-section of crimped sample*

In the area at point A of the cross-section, due to the effect of the gap of the field shaper as shown in Fig. 5(a), the terminal and the HV wire harness are not integrated. In the crimping process, the Lorentz force F induced in the Cu terminal is given by Eq. 3.

$$F = J \times \left(B_{\mathrm{J}} + B_{\mathrm{d}} \right) \tag{3}$$

where J is the induced eddy current of the terminal. As shown in Fig. 5(b), B_J is the magnetic induction sum of the induced eddy current magnetic induction B_{J2} on the outer surface and the induced eddy current magnetic intensity on the inner surface B_{J1}. B_d is the magnetic induction produced by the discharge current.

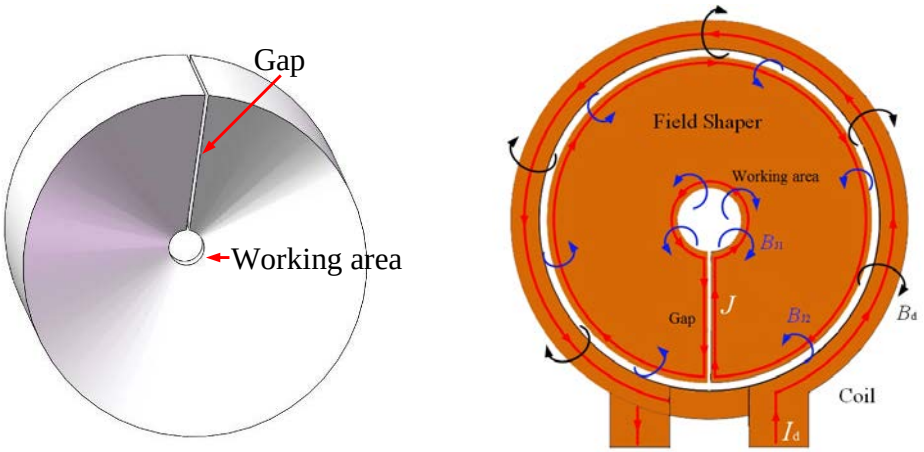

(a) (b)

Figure 5*: (a) Geometry of the field shaper, and (b) magnetic induction direction.*

The diameter of the crimping coil is large, so the distance between the working area of the field shaper and the coil is large. Therefore, the magnetic induction intensity B_d generated by the discharge current has a small effect on the Lorentz force. And the Lorentz force is mainly affected by the induced eddy current in the working area of the field shaper. Because of the gap in the field shaper, there is no magnetic induction produced in this area. The Lorentz force cannot be generated on the copper terminal corresponding to this gap area. The relationship between Lorentz force and terminal deformation can be expressed as

$$\rho \frac{\partial^2 \boldsymbol{s}}{\partial t^2} - \nabla \cdot \sigma = \boldsymbol{f} \tag{4}$$

where ρ is the density of the terminal. $\boldsymbol{s}$ is the displacement vector. σ is the stress tensor and $\boldsymbol{f}$ is the Lorentz force density. The deformation of the area of the terminal corresponding to the gap is caused by the deformation of other areas, and the amount of deformation is small. Under the influence of the gap, the amount of deformation near the gap is lower than that far away from the gap. Thus, different effects appeared at the interface of the crimped sample.

4.2 Micromorphology analysis

Area B and area C on the cross-section of the crimped sample in Fig. 4(b) were taken for micromorphology analysis, which is near area A and far away from area A, respectively. The scanning electron microscope (SEM) images for the area B and area C are presented in Fig. 6. There is a continuous flat coating between the Cu terminal and the Cu wire harness

as presented in Fig. 6(a), but there are also some nicks in the coating layer. On the surface of the Cu terminal, there are some scattered spots, which are consistent with the color of the coating layer, showing the coating layer destroyed and entering the inside of the Cu terminal in the crimping process.

There is a clear continuous coating layer with the characteristic waviness of EMPC in area C as shown in Fig. 6(b). It indicated that the height of the wave can be 8.81 μm, and the length of the wave can be 115.79 μm. The wavy shape increases the contact area of the joint and mechanically interlocks to produce a strong bond. There are the flat interface and the wavy interface at the same joint. Due to the existence of the gap in the field shaper, the Lorenz force in the radial direction is different. Thus, the force on the entire circumference and the deformation of the Cu terminal are inconsistent. The Lorentz force near the gap of the field shaper is smaller, and the Lorentz force far away from the gap of the field shaper is larger. The formation of the waveform is related to the collision speed. The higher the collision speed, the easier it is to produce the wavy interface. Therefore, there are a flat interface and a wavy interface at the connection interface. Moreover, there are also tiny nicks in the coating. On the surface of the Cu terminal, some intermittent coating layers are consistent with the color of the continuous coating layer, showing the coating layer is destroyed and enters the inside of the Cu terminal in the forming process of the wavy interface. Compared with the flat interface, the intermittent coating layers of the wavy interface is longer more obvious, because the collision of the wavy interface is more violent.

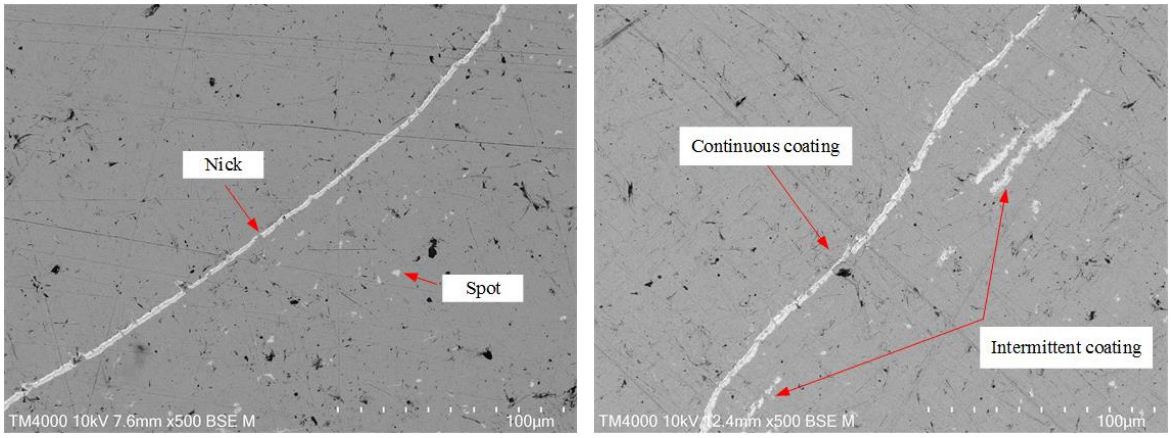

(a) (b)

***Figure 6**: (a) Micromorphology of the flat interface, and (b) Micromorphology of the wavy interface*

4.3 Element distribution analysis

To further study the composition of the interface that is different from the Cu terminal and Cu wire harnesses, the distribution of elements was analyzed by EDS. Fig. 7(a) shows the position of line 1 in the flat interface, and it is about 40 μm and the line scan result of the crimped sample is presented in Fig. 7(b). There is no platform area between the Cu wire

harness and the Cu terminal, indicating that no intermetallic compounds are produced in the crimping process, or there are few metal compounds, which are difficult to detect. Moreover, Ag and Sn exist in the zone between the Cu terminal and Cu wire harnesses, forming a boundary. And the width of the coating layer is about 2 μm. Fig. 8(b) is the position of line 2 in the wavy interface, which is about 32 μm. There is also no platform area between the Cu wire harness and the Cu terminal, indicating that no intermetallic compounds are produced in the crimping process. The Ag coating layer and Sn coating layer are still between the Cu terminal and Cu wire harnesses, and the width of the coating layer is about 4 μm. The coating layer of the wavy interface is thicker than that of the flat interface because there is a nick on the coating layer of the flat interface as shown in Fig. 6(a), showing it is damaged during the crimping process. The huge impact pressure makes the metals form a metallurgical bond, and the metals are embedded in each other. In this process, the coating layer is deformed and displaced. And the coating layer is not destroyed, which is related to the energy and angle of the collision. The coating layer on the wavy interface is also damaged.

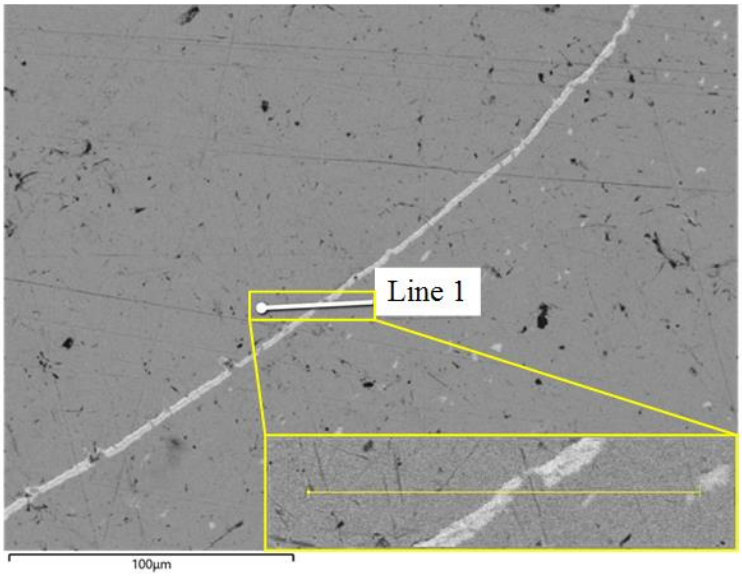

(a)

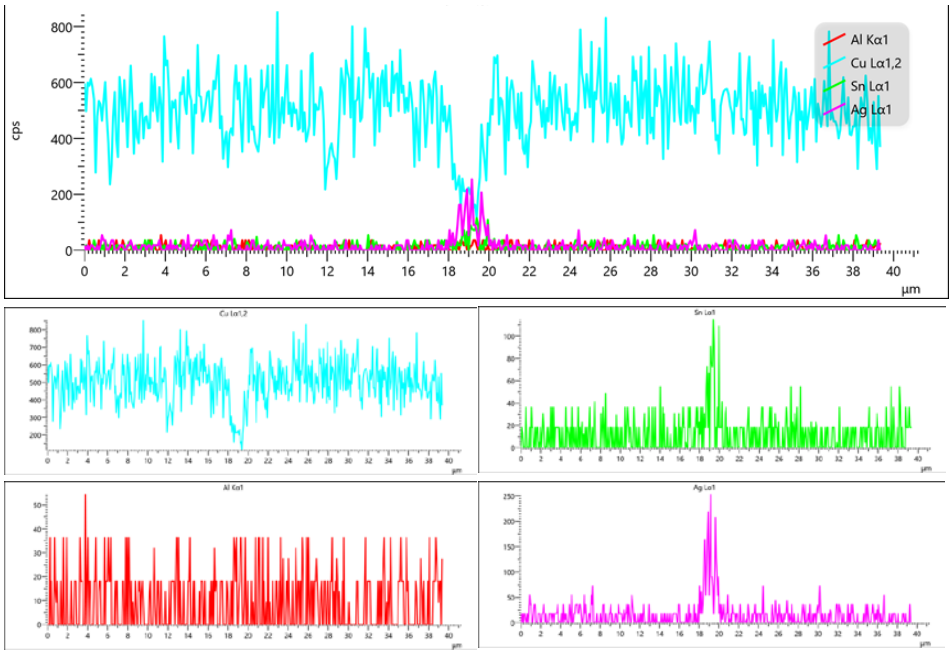

(b)

***Figure 7**: (a) EDS analysis area of the flat interface, and (b) EDS analysis result of the wavy interface*

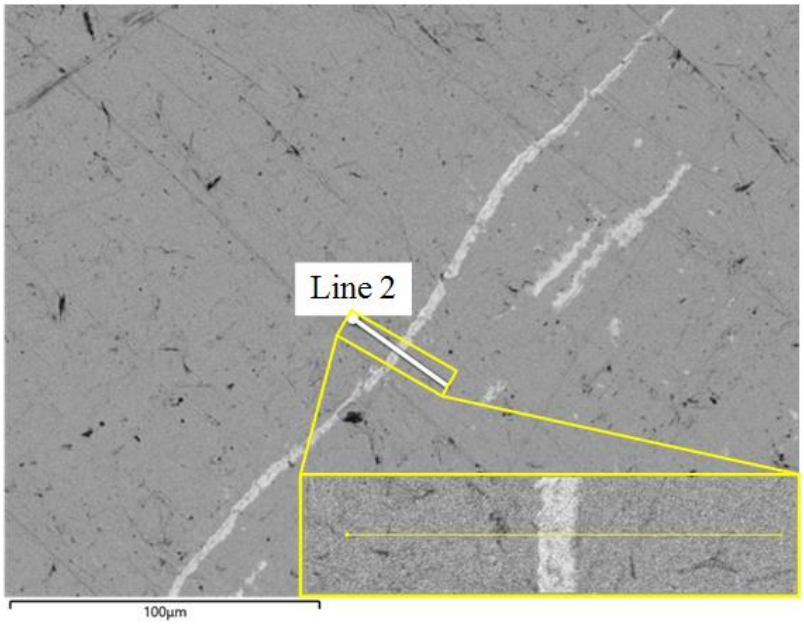

(a)

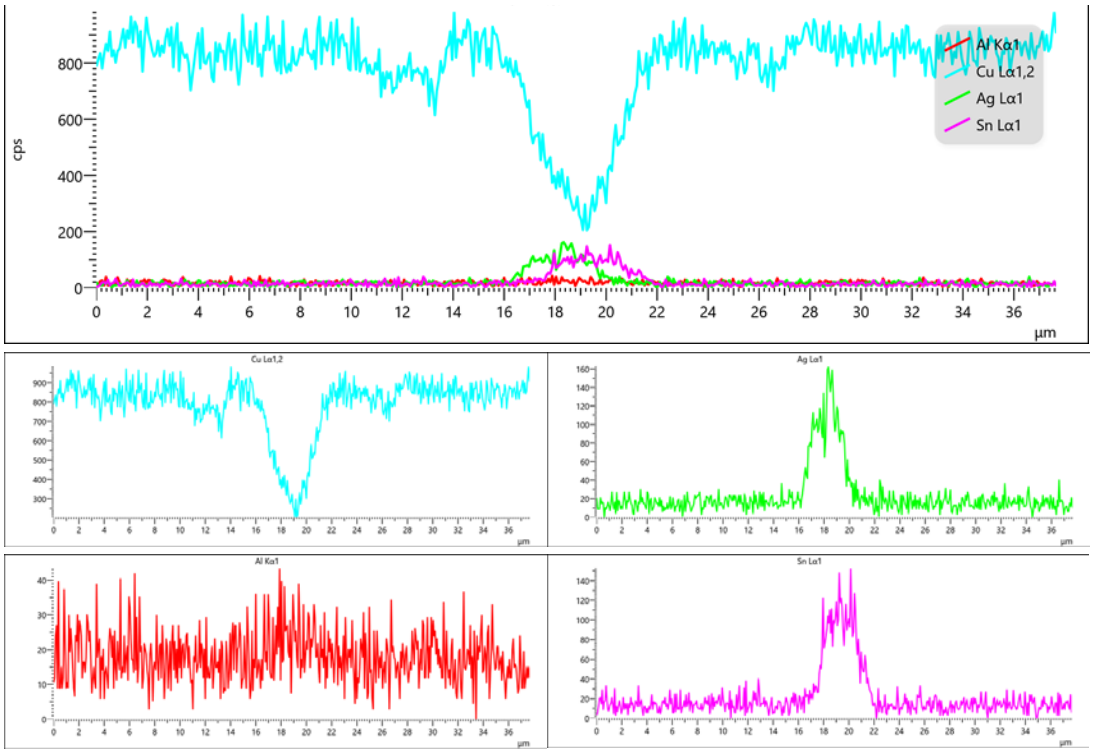

(b)

***Figure 8**: (a) EDS analysis area of the wavy interface, and (b) EDS analysis result of the wavy interface*

Fig. 4(b) shows that there is no obvious boundary on the surface of the Cu wire harnesses. To explore the connection performance between Cu wire harnesses, surface scanning is used to analyze the interface between Cu wire harnesses and Cu wire harnesses. The observation area is shown in Fig. 9(a). The area of this region is about 2.61 mm × 1.94 mm, which is larger than the diameter of each strand of 0.46 mm. The surface scanning results are shown in Fig. 9(b), there are Cu, C, and O. Cu is evenly distributed across the observation interface, and the metallurgical bond is formed between the Cu wire and the Cu wire. Carbon is brought in during the sanding process. Oxygen is brought in by the combination of Cu and oxygen in the air.

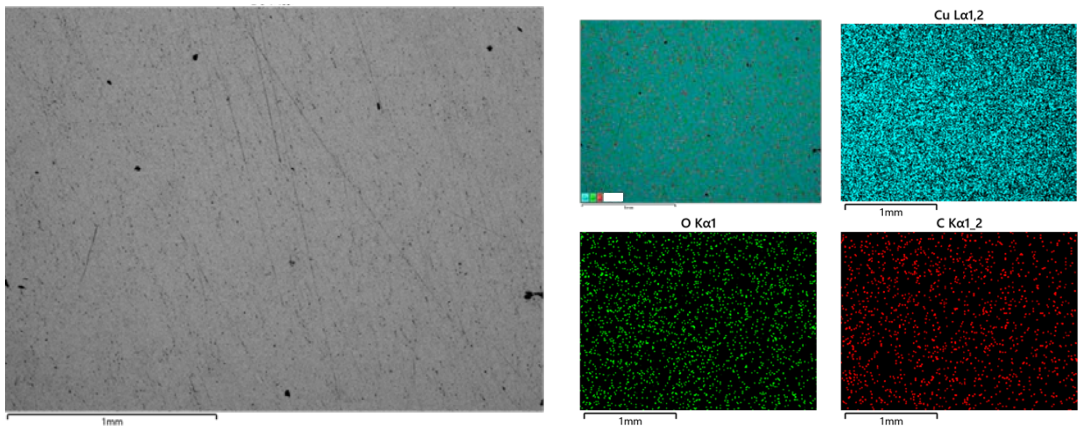

(a) (b)

***Figure 9**: (a) Micromorphology of the harness interface, and (b) EDS analysis result of the harness interface*

5 Conclusion

The reliable connection between the HV wire harness and the terminal is of great significance to the energy transmission and safety performance of EVs. Aiming at the difficult problem of obtaining a reliable connection between Cu HV wire harness and Cu terminal, this work proposes to use the EMPC technology to crimp the Cu HV wire harness and Cu terminal. A 28 kJ EMPC system has been designed, developed, and built. And the crimping experiments and tests of the Cu wire harnesses and Cu terminals have been carried out. Draw the following conclusions from this work:

1) The metallurgical joint was obtained through the EMPC experiment between Cu wire harnesses and the Cu terminal under the discharge voltage of 13 kV. The compression ratio is about 85% in the contact area, which meets the relevant standards.

2) The peak value of the discharge current is about 70 kA when the discharge voltage is 13 kV, and the frequency is about 5.6 kHz. There is no obvious effect of the temperature rise on the coating of the Cu terminal in the crimping process.

3) There are the flat interface and wavy interface between the Cu wire harnesses and the Cu terminal, which indicates that the two have formed a metallurgical bond. The different interface morphology is caused by the gap of the field shaper. Moreover, metallurgical bonding has also been obtained between the Cu wire harnesses.

Acknowledgments

This work was supported by graduate research and innovation foundation of Chongqing, China (Grant No.CYB20017), which is gratefully acknowledged here.

References

Cao Q., Han X., Lai Z., Xiong Q., Zhang X., Chen Q., Xiao H., Li L., 2015 *Analysis and reduction of coil temperature rise in electromagnetic forming*. Journal of Materials Processing Technology 225, pp. 185-194.

Engr, B., Iek, A., Erenolu, A.K., Erdin, O., Catalo, J., 2020. *User-comfort oriented optimal bidding strategy of an electric vehicle aggregator in day-ahead and reserve markets*. International Journal of Electrical Power & Energy Systems, 122, 106194.

Itoi, T., Inoue, S., Nakamura, K., Kitta, S., Okagawa, K., 2018. *Lap joint of 6061 aluminum alloy sheet and dp590 steel sheet by magnetic pulse welding and characterization of its interfacial microstructure*. Journal of Japan Institute of Light Metals, 68(3), pp. 141-148.

Lopes, J.A.P., Soares, F.J., Almeida, P.M.R., 2011. *Integration of electric vehicles in the electric power system*. Proceedings of the IEEE, 99 (1), pp. 168-183.

Psyk, V., Risch, D., Kinsey, B.L., Tekkaya, A.E., Kleiner, M., 2011. *Electromagnetic forming – A review*. Journal of Materials Processing Technology 211 (5), pp. 787-829.

Rajak, A. K., and Kore, S. D., 2018. *Numerical simulation and experimental study on electromagnetic crimping of aluminium terminal to copper wire strands*. Electric Power Systems Research 163, pp. 744-753.

Shotri, R., Faes, K., De, A., 2020. *Magnetic pulse welding of copper to steel tubes–experimental investigation and process modelling*. Journal of Manufacturing Processes, 58, pp. 249-258.

Zhou, Y., Zhou, Z., Yao, C., Tan, J., Wang, X., Wang, C., Hu, Y., Yang, G., 2017. *Fast-rise-time trigger source based on solid-state switch and pulse transformer for triggered vacuum switch*. IEEE Transactions on Dielectrics & Electrical Insulation, 24(4), pp. 2105-2114.

Zhou, Y., Li, C., Wang, X., Liao, Z., Shi, X., Yao, C., 2021. *Investigation of flyer plate dynamic behavior in electromagnetic pulse welding*. Journal of Manufacturing Processes, 68, pp. 189-197.